Received: 9 November 2019 | Revised: 16 February 2020 | Accepted: 22 February 2020

DOI: 10.1002/app.49218

ARTICLE

Applied Polymer SCIENCE WILEY

Curing behavior of a UV-curable inkjet ink: Distinction between surface-cure and deep-cure performance

Jonas Simon[1] | **Andreas Langenscheidt**[2]

[1]Goethe University Frankfurt, Frankfurt am Main, Germany

[2]Tritron GmbH, Battenberg (Eder), Germany

Correspondence
J. Simon, Goethe University Frankfurt, 60438 Frankfurt am Main, Germany.
Email: j.simon@stud.uni-frankfurt.de

Abstract

Safety requirements and the need of low-migration UV inks have received increasing attention in the packaging industry. Crucial for the development and design of low-migration UV inkjet inks for migration-sensitive applications is the polymerization degree. In this study, curing-behavior of a black, high purity packaging ink (HPP-ink) was monitored using ATR-FTIR spectroscopy. UV irradiation of HPP-ink led to changes in specific absorption bands of the FTIR spectra due to crosslinking reaction of double bonds. Changes in absorptions bands at 1,408 and 1,321 cm^{-1} permitted the determination of C=C conversion of acrylic and vinyl double bond, independently of one another. In addition, a method was developed which allows the investigation of surface-cure and deep-cure behavior, separately.

KEYWORDS

ATR-FTIR, packaging, photochemistry, photopolymerization

1 | INTRODUCTION

For packing applications and labeling with the inkjet printing process, the industry is predominantly using UV curable printing inks. UV curable inkjet printing systems are best suited for packaging printing because they combine high productivity and substrate diversity, including rigid and flexible plastics. However, UV curable inks are used for migration-sensitive applications such as food, health care, personal care, and tobacco.[1,2] Safety requirements and the need of low-migration UV inks has received an enormous amount of interest in recent years.[3–6] UV inks often do not fulfill guidelines established to regulate low-migration inks due to viscosity limitations. Crucial for the development and design of low-migration UV inkjet inks for migration-sensitive applications is the polymerization degree. If the ink is not sufficiently cured, free unreacted monomers with low-molecular-weight tend to migrate through the substrate, unless the substrate is an absolute migration barrier.[7,8] In addition, photoinitiators used in standard UV inkjet inks are also low-molecular-weight molecules and thereby are not designed for migration-sensitive applications.[9,10] Low-migration inks for alternative printing techniques, such as flexo and offset, circumvent the problem by using multifunctional polymerizable compounds and photoinitiators with a molecular weight of above 1,000 Da, thereby limiting the risk of migration.[11] For inkjet printing, the viscosity shall be low enough to allow for firing through the orifice of the print head nozzles, and therefore it is impossible to use only high-molecular-weight ink compounds.[1] The development of low-migration UV curable inkjet inks requires to increase the degree of double bond conversion by using polyfunctional and highly reactive monomers combined with photoinitiators which are either implicitly less sensitive to migrate or supported by sufficient toxicological data to allow relatively high amounts to migrate.[11]

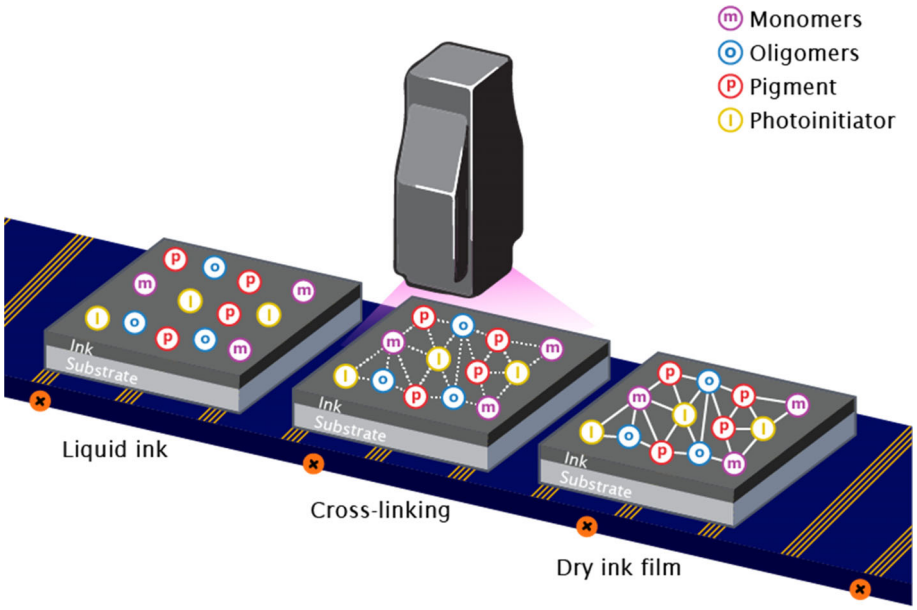

FIGURE 1 Drying process of UV curable inks. Liquid ink is transformed into a polymerized solid initiated by UV-exposure. The UV dosage is varied by adjusting the speed of the conveyor system [Color figure can be viewed at wileyonlinelibrary.com]

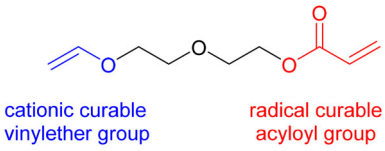

FIGURE 2 Chemical structure of VEEA. VEEA combines a radical polymerizable acryloyl group and a cationic polymerizable vinylether group in one molecule [Color figure can be viewed at wileyonlinelibrary.com]

UV curing is a radiation curing process and involves solid film formation through crosslinking and polymerization (Figure 1).[12] Compared to thermal polymerization methods, which usually require elevated temperatures, photopolymerization can be initiated at room temperature. UV curing is a photochemical process in which high-intensity UV radiation is used to instantly cure inks and coatings. The polymerization takes place usually in fractions of a second.[13,14] In general, there are essentially two different mechanisms that UV curing may occur by—free radical and ionic, predominantly cationic.[12,15,16]

Curing behavior of UV curable printing inks can be monitored using Fourier transform infrared (FTIR) spectroscopy.[17,18] FTIR spectroscopy is one of the most widely employed techniques for analyzing polymeric materials.[19] It is most commonly used in its multiple reflection mode (ATR) which enables samples to be examined directly in the solid or liquid state without further preparation.[20] Thus, ATR-FTIR allows tracking of double bond conversion in crosslinking and photopolymerization reactions. Although the penetration depth is only about 1 µm, so far no distinction has been made between surface-cure and deep-cure performance.[21–23] Alternatively, nanoindentation is a powerful tool for investigating

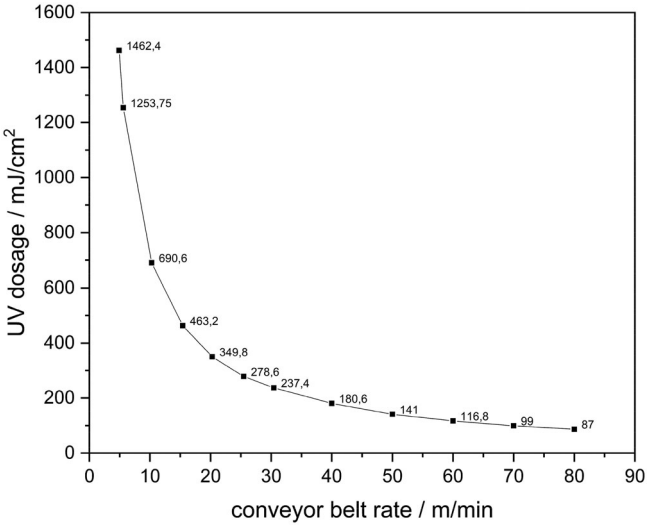

FIGURE 3 UV dosage of Phoseon FireJet FJ 200 air-cooled UV LED light source depending on the velocity of the conveyor system

mechanical properties of coatings and films, and has been reported as a method to evaluate the curing behavior of a UV-curable inkjet ink.[24–28] Although this method allows to measure the hardness of cured films, it does not permit the analysis of the conversion rate of acrylic and vinyl double bonds independently. However, the knowledge is essential to improve the properties of the ink, since they react according to different mechanisms.[12,15,16]

In this study, curing-behavior of a black, high purity packaging ink (HPP-ink) was monitored using ATR-FTIR spectroscopy. The overarching aims of the research were twofold: (a) To examine the effect of UV-dosage on both surface-cure and deep-cure performance; (b) To evaluate the conversion rate of acrylic and vinyl double bonds independently. For this purpose, the light source used

was first characterized and the observed absorption bands were assigned to certain vibrations.

2 | EXPERIMENTAL

2.1 | Instruments

Infrared analysis of the UV curable inkjet ink (HPP-ink) and the corresponding cured films were performed on a Bruker ALPHA II FTIR spectrometer. The internal reflection element was a diamond crystal and its reflective index was 2.4. The angle of incidence on the crystal was set to 45°. The parameters for all analyses conducted include a resolution of 4 cm^{-1}, spectral range of 4,000–400 cm^{-1}, and 23 scans per sample. The depth of analysis is about 1 µm. Bruker's spectroscopy software OPUS (v 8.2.21) was used for processing and evaluation of FTIR spectra. All results were obtained with a baseline correction and reproduced at least three times to eliminate outliers. OriginPro (v 2018b 9.55) was used for graphical representation and analysis of measured data. Irradiation with UV LED light was performed with a Phoseon FireJet FJ 200 air-cooled UV LED light source ($\lambda = 395$ nm). A working distance of 5.2 mm for the LED units was selected. The UV dosage was varied by adjusting the speed of the conveyor system and measured with an Opsytec Dr. Gröbel UVpad spectral radiometer.

2.2 | Materials

The UV curable inkjet ink used (HPP-ink) was developed and provided by Tritron GmbH (Battenberg, Germany). The composition mainly contains 2-(2-vinyloxyethoxy)ethyl acrylate (VEEA) (Figure 2), acrylates, photoinitiators, carbon black pigment and various kinds of additives. Diethylene glycol monoethyl ether acetate was obtained from Fluka and 2-(2-ethoxyethoxy)ethyl acrylate was purchased from TCI. All the chemicals were used as received without further purification. Plastic cards (PVC, 6 cm × 10 cm) and polished stainless steel (6 cm × 10 cm) were chosen as the substrates in investigations on the curing behavior of HPP-ink. Samples were prepared using the K Hand Coater (9 µm, RK PrintCoat Instruments Ltd.).

TABLE 1 UV intensity *I* of Phoseon FireJet FJ 200 in the experimental setup

Phoseon FireJet FJ 200 (working distance $h = 0.52$ mm)		
UV dosage/mJ/cm²	*t*/s	*I*/W/cm²
1,462.4	0.244	5.993
1,253.8	0.214	5.859
690.6	0.117	5.903
463.2	0.078	5.938
349.8	0.059	5.929
278.6	0.047	5.928
237.4	0.039	6.087
180.6	0.030	6.020
141.0	0.024	5.875
116.8	0.020	5.840
99.0	0.017	5.824
87.0	0.015	5.800

2.3 | FTIR measurements

The curing behavior of HPP-ink was analyzed by observing changes in the conversion of the C=C bonds. The relevant IR bands were determined and assigned by comparison with IR spectra of selected reference materials. Thus, IR spectra of uncured HPP-ink, VEEA, diethylene glycol monoethyl ether acetate and 2-(2-ethoxyethoxy)ethyl

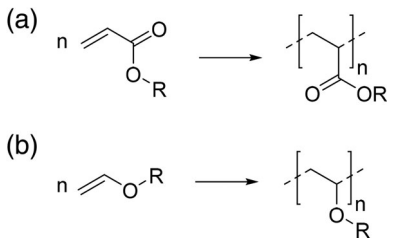

FIGURE 4 Depiction of double bond conversion during the curing process in (a) acryloyl group and (b) vinylether group

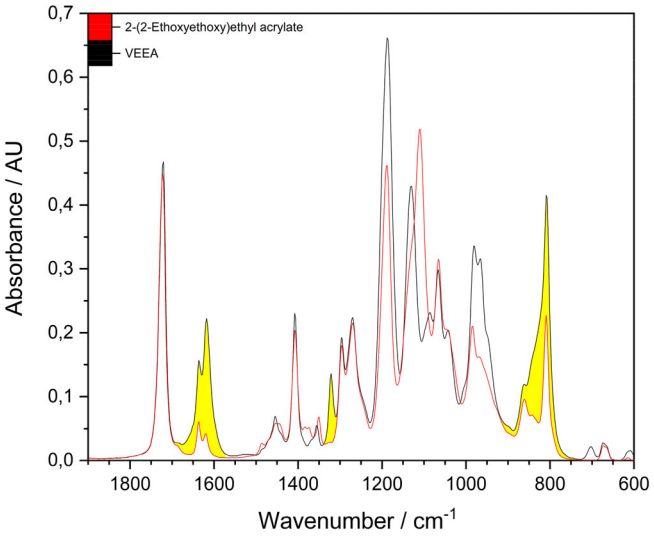

FIGURE 5 FTIR spectra of VEEA (——) and 2-(2-ethoxyethoxy)ethyl acrylate (——). Significant differences are represented by the yellow areas [Color figure can be viewed at wileyonlinelibrary.com]

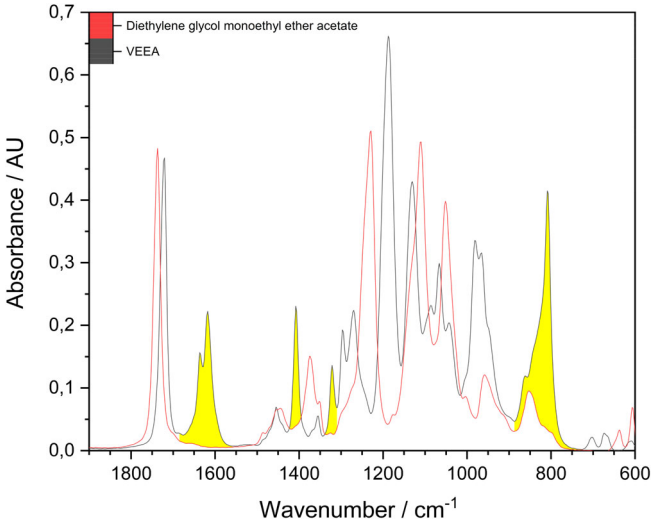

FIGURE 6 FTIR spectra of VEEA (——) and Diethylene glycol monoethyl ether acetate (——). Significant differences are represented by the yellow areas [Color figure can be viewed at wileyonlinelibrary.com]

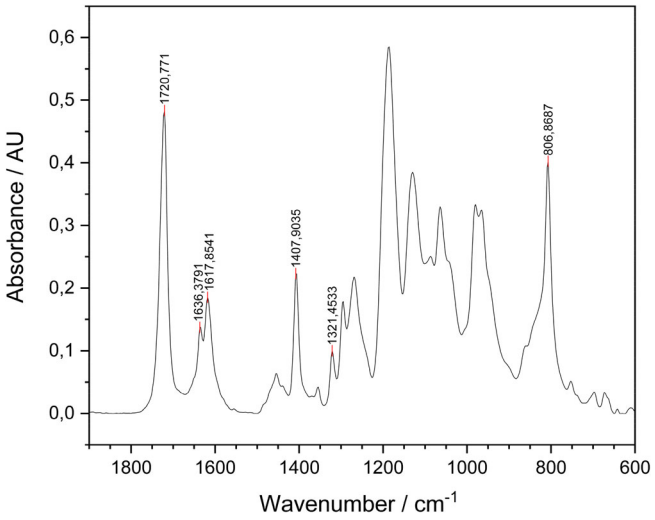

FIGURE 7 FTIR spectra of uncured HPP-ink, including peak picking and assignment of relevant absorption bands [Color figure can be viewed at wileyonlinelibrary.com]

acrylate were recorded. Selected liquid samples were placed on the ATR crystal without additional preparation. Absorbance measurements with the ART-FTIR spectrometer were performed with samples of 9 µm thickness (3 cm × 9 cm), which corresponds to common layer thickness in inkjet printing. Samples were prepared by coating HPP-ink on a PVC or polished stainless steel substrate using the K Hand Coater, which produce a uniform and repeatable coating. For deep-cure investigations, the cured film was peeled off a polished stainless steel substrate using a tesafilm® stripe due to poor adhesion properties on stainless steel surfaces. The reverse side of the film was analyzed. Samples were mounted in the sample holder and no additional sample preparation was done. The front and the back of the cured ink films were analyzed at different UV dosages. Both, surface-cure and deep-cure behavior were observed in a UV dose range of 80–1,500 mJ/cm^2.

TABLE 2 Attribution of main bands in FTIR spectra of HPP-ink

Peak position	Assignment
1,721 cm^{-1}	C═O stretching vibration
1,618–1,636 cm^{-1}	C═C stretching
1,408 cm^{-1}	═C—C═O vibration
1,321 cm^{-1}	═C—O bending vibration
807 cm^{-1}	C═C twisting vibration

3 | RESULTS AND DISCUSSION

3.1 | UV intensity and UV dosage

The easiest way to change the UV dosage is by changing the speed of the conveyor system. Conversion rates of UV curable inkjet inks are governed by the irradiated UV dosage. When the UV dosage is assigned to a conveyor velocity, ATR-FTIR spectroscopy permits to determine the actual degree of conversion at a certain amount of irradiated energy. For this reason, the UV dosage was recorded at varying velocity of the conveyor system. The dependency of irradiated UV dosage on the velocity of the conveyor system is demonstrated in Figure 3.

The data unequivocally demonstrate that UV dosage decreases reciprocally with increasing velocity of the conveyor system, and thus with reducing irradiation time. The UV dosage depends on the intensity of UV radiation I (W/cm^2) and exposure time t (s) and thus is expressed in J/cm^2. This leads to the following equation for the UV dosage:

$$\text{UV dosage}\left(\text{J/cm}^2\right) = \text{I}\left(\text{W/cm}^2\right) \cdot \text{t}\,(\text{s}) \qquad (1)$$

All exposure processes can be easily defined by UV dosage. Matching of velocity and UV dosage permits the optimization of curing processes and efficiency. Introducing this expression in Equation (1) leads to the following equation for the UV intensity I:

$$\text{I}\left(\text{W/cm}^2\right) = \frac{\text{UV dosage}}{t} = \frac{\text{UV dosage} \cdot v}{s} \qquad (2)$$

Here, t is the exposure time, v the velocity of the conveyor system, and s the path length of radiation exposure. The path length s is measured to be 2.0 cm for Phoseon

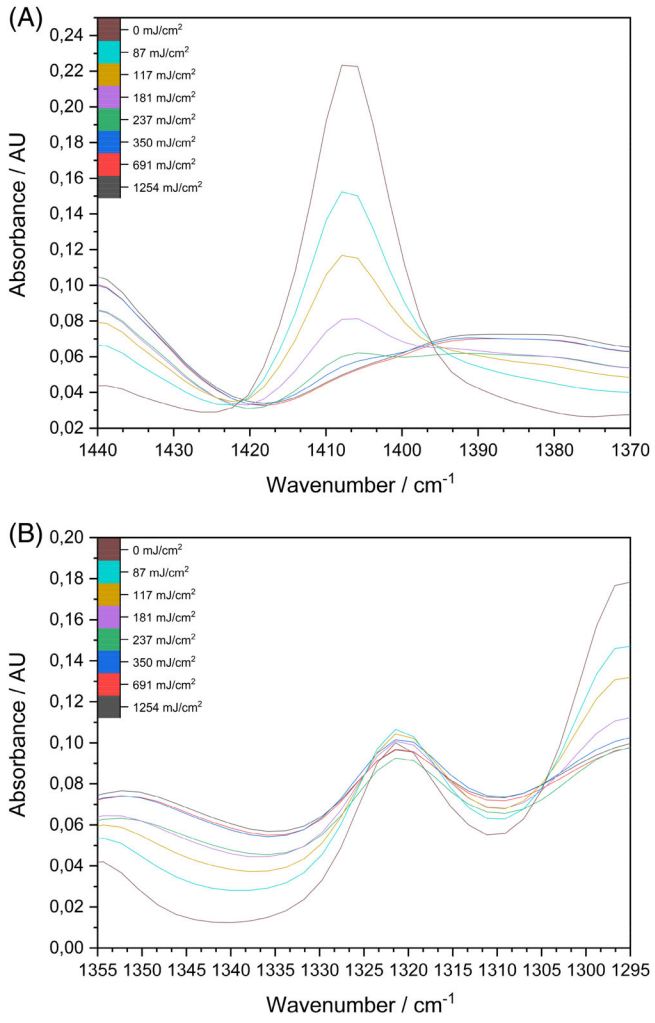

FIGURE 8 FTIR spectra of HPP-ink at (a) 1,408 cm^{-1} and (b) 1,321 cm^{-1}, before and after exposure to radiation from UV LED light source (395 nm) for different UV dosages: (——) 0, (——) 87, (——) 117, (——) 181, (——) 237, (——) 350, (——) 691, (——) 1,254 mJ/cm^2, respectively [Color figure can be viewed at wileyonlinelibrary.com]

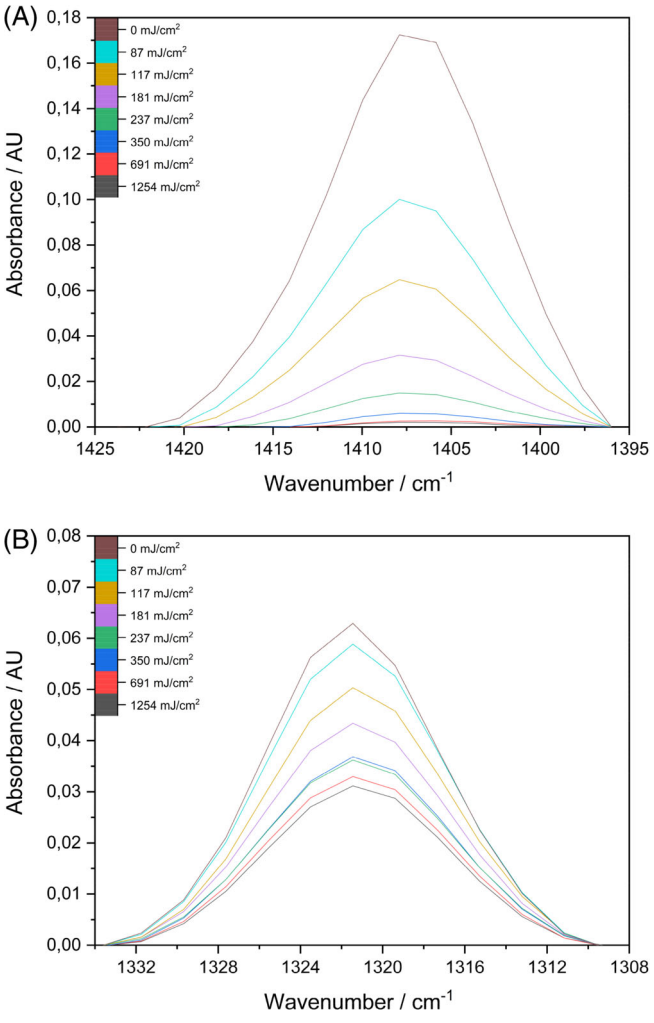

FIGURE 9 Baseline subtracted FTIR spectra of HPP-ink at (a) 1,408 cm^{-1} and (b) 1,321 cm^{-1}, before and after exposure to radiation from UV LED light source (395 nm) for different UV dosages: (——) 0, (——) 87, (——) 117, (——) 181, (——) 237, (——) 350, (——) 691, (——) 1,254 mJ/cm^2, respectively [Color figure can be viewed at wileyonlinelibrary.com]

FireJet FJ 200. The *s* values can be used to calculate the UV intensity using Equation (2). The UV intensity of the light source used is presented in Table 1.

It can be clearly observed from Table 1 that at constant working distance *h*, constant intensity is determined. Slight deviations in *I* between individual measurements (Table 1) can be attributed to Gaussian distribution of intensity in width and statistical deviations of the used spectral radiometer.

3.2 | Selection and correlation of IR bands

ATR-FTIR spectroscopy was used to monitor the curing process of HPP-ink. As noted, HPP-ink mainly contains VEEA, acylates, photoinitiators, carbon black pigment and various kinds of additives. Thus, the system compromises two types of double bonds that react according to different mechanisms—a radically polymerizable acryloyl group and a cationically and radically polymerizable vinylether group. With the curing process going on, both types of double bond being consumed (Figure 4).

In this research work, the conversion of both types of double bond was investigated independently. This requires an assignment of signals to certain vibrations. FTIR reference spectra of VEEA and 2-(2-ethoxyethoxy) ethyl acrylate are shown in Figure 5. VEEA and 2-(2-ethoxyethoxy)ethyl acrylate differ only in a vinylic double bond. It was found that both compounds showed

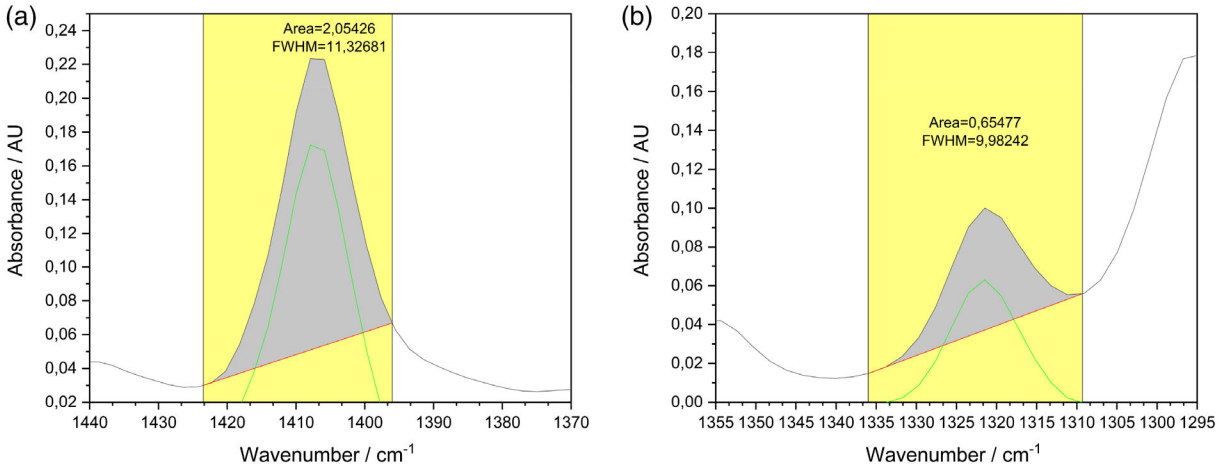

FIGURE 10 Integration of the absorption bands at 1408 cm^{-1} in (a) and 1,321 cm^{-1} in (b) of uncured HPP-ink [Color figure can be viewed at wileyonlinelibrary.com]

TABLE 3 Percent conversion *X* of acrylic and vinyl C═C bond of HPP-ink for different UV dosages

Acrylic C═C (1,408 cm^{-1})			Vinyl C═C (1,321 cm^{-1})		
UV dosage/mJ/cm²	A_{1408}	*X*/%	**UV dosage/mJ/cm²**	A_{1321}	*X*/%
0	2.054	0.0	0	0.655	0.0
87	1.181	42.5	87	0.625	4.6
117	0.747	63.6	117	0.539	17.8
181	0.350	83.0	181	0.470	28.2
237	0.157	92.3	237	0.396	39.5
350	0.055	97.3	350	0.399	39.1
691	0.026	98.8	691	0.356	45.7
1,254	0.018	99.1	1,254	0.333	49.1

absorption bands at 1,636 cm^{-1}, 1,618 cm^{-1} and 807 cm^{-1} which significantly decreased for 2-(2-ethoxyethoxy)ethyl acrylate. This indicates that both C═C vibrations superpose in the mentioned wavelength regions. However, the absorption band at 1,321 cm^{-1} is visible for VEEA only and thus is due to ═C—O— bonding vibration.

Figure 6 shows the FTIR spectra of VEEA and diethylene glycol monoethyl ether acetate. Diethylene glycol monoethyl ether acetate contains neither acrylic double bond nor vinyl double bond. Thus, absorption bands at 1636 cm^{-1}, 1,618 cm^{-1}, 1,408 cm^{-1} 1,321 cm^{-1}, and 807 cm^{-1} are not visible.

Consequently, the absorption band at 1,408 cm^{-1} is due to acrylate group. The C═O stretching vibration around 1,721 cm^{-1} appears in all three spectra (Figure 5 and 6). Based on the analyzed FTIR reference spectra, Figure 7 shows the FTIR spectra of uncured HPP-ink, including assignment of relevant absorption bands (Table 2).[29,30]

3.3 | Curing behavior monitored by ATR-FTIR

In this study, UV curing behavior was determined by integrating the absorbance peaks around 1,408 cm^{-1} and 1,321 cm^{-1}. Several studies have shown that the adsorption band at 807 cm^{-1} due to C═C twisting vibration and at 1618 to 1,636 cm^{-1} due to C═C stretching decreases with UV exposure time.[29,30] However, both acrylic and vinyl double bond absorb at 807 cm^{-1} and at 1,618 to 1,636 cm^{-1}. Thus, the changes in absorption bands are due to crosslinking reactions of both double bond types. Investigation of the absorption band at 1,408 and 1,321 cm^{-1} permits the determination of C═C conversion of acrylic and vinyl double bond, independently of one another. Figure 8 shows the FTIR spectra of HPP-ink, before and after exposure to radiation from 395 nm LED light source for various UV dosages in relevant spectral regions. The UV dosage was

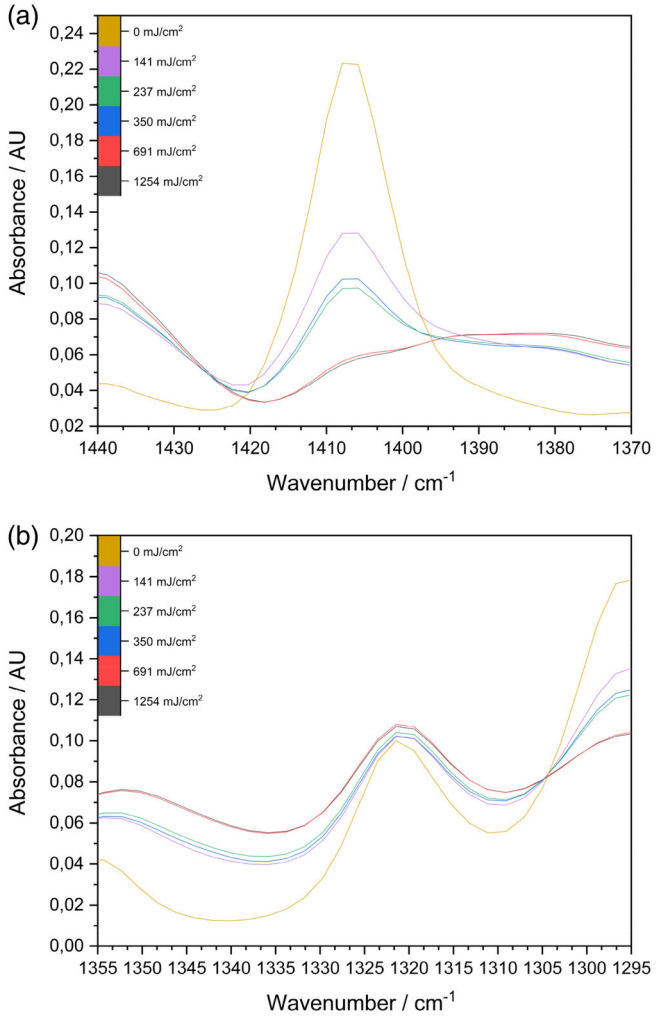

FIGURE 11 FTIR spectra of the back side of HPP-ink at (a) 1,408 cm^{-1} and b) 1,321 cm^{-1}, before and after exposure to radiation from UV LED light source (395 nm) for different UV dosages: (——) 0, (——) 141, (——) 237, (——) 350, (——) 691, (——) 1,254 mJ/cm^2, respectively [Color figure can be viewed at wileyonlinelibrary.com]

varied by adjusting the speed of the conveyor system. The front side of the film was analyzed (film thickness: 9 μm; substrate: PVC).

UV irradiation of HPP-ink leads to changes in specific absorption bands of the FTIR spectra due to crosslinking reaction of double bonds. The peak absorbances due to acrylic double bond (Figure 8a) and vinyl double bond (Figure 8b) are reduced with increasing UV dosage. The double bond conversion due to UV exposure and the related decrease in absorption bands is more significant for baseline subtracted peaks. The corresponding baseline subtracted FTIR spectra of HPP-ink are shown in Figure 9.

The curing performance and the curing rate can be demonstrated by integrating the absorbance peaks. Peak integration and baseline subtraction using OriginPro (v 2018b 9.55) enables the calculation of percentage decrease of the absorbance peaks, and thus the conversion in percent. The limits of integration need to be specified for integration between two absorption minima. Due to peak overlapping of the absorbance peak around 1,408 cm^{-1} (Figure 8 a)) the right hand limit is set to 1,396.00 cm^{-1}, equivalent to an isosbestic point. The integration of absorbance peaks around 1,408 and 1,321 cm^{-1} are depicted in Figure 10—exemplary for uncured HPP-ink.

The integrated areas in Figure 10 are assumed to be equivalent to the presence of no C═C conversion. The conversion X was calculated according to the following equation:

$$X(\%) = 100 - \frac{A_{\tilde{\upsilon}} \cdot 100}{A_0} \quad (3)$$

where $A_{\tilde{\upsilon}}$ is the integral of the corresponding peak at a specific wavenumber $\tilde{\upsilon}$ and A_0 is the corresponding integral before UV irradiation. Double bond conversion X for acrylic and vinyl C═C bond of HPP-ink due to UV irradiation are listed in Table 3.

It can be seen from Table 3 that as the UV dosage increases, the conversion of acrylic double bonds increases very fast in the area of small UV dosages and then becoming more and more constant. At 691 mJ/cm^2 the acrylic portion of C═C double bonds is almost completed, but even at 1254 mJ/cm^2 it did not reach 100%. Joo and coworkers shared similar results investigating the curing performance of UV-curable acrylic binders.[30] The remaining double bonds might have remained unreacted because they were trapped in the cured polymer network. The reactivity of vinyl C═C bonds is markedly weaker. At 1,254 mJ/cm^2 almost half of the vinyl double bonds were crosslinked by photopolymerization. Introducing cationic photoinitiators could lead to an increase in conversion.

Investigations of the front side of the cured film via ART FTIR spectroscopy do not provide information about the deep curing performance of the UV curable inkjet ink. Due to a penetration depth of about 1 μm, only a fraction of the 9 μm thick film is examined. Hence, deep-cure behavior of HPP-ink was investigated by peeling of the cured film and analyzing the reverse side of the crosslinked system. Figure 11 shows the specific peaks at 1408 cm^{-1} and 1,321 cm^{-1} of the reversed side after UV exposure of about 395 nm for various UV dosages. The processing of the data and integration of the peaks was carried out analogously to Figure 10. The C═C conversion is calculated according to Equation 3 (Table 4). As seen for the front side of the cured ink film, the absorption bands at 1,408 cm^{-1} and 1,321 cm^{-1} went down

TABLE 4 Percent conversion X of the back of HPP-ink for different UV dosages

Acrylic C=C (1,408 cm^{-1})			Vinyl C=C (1,321 cm^{-1})		
UV dosage/mJ/cm^2	A_{1408}	X/%	UV dosage/mJ/cm^2	A_{1321}	X/%
0	2.054	0.0	0	0.655	0.0
141	0.774	62.3	141	0.505	23.0
237	0.458	77.7	237	0.501	23.6
350	0.529	74.3	350	0.488	25.5
691	0.076	96.3	691	0.471	28.1
1,254	0.037	98.2	1,254	0.457	30.2

gradually with increasing UV exposure. However, sufficient conversion of the acrylic double bond is only observed at an irradiated UV dosage of 691 mJ/cm^2 and more. A comparable curing performance was achieved on the front at half the UV dosage (350 mJ/cm^2). On the other hand, the conversion of the vinyl double bond reached only 30% at an irradiated UV dosage of 1,254 mJ/cm^2. Moreover, it is striking that the vinyl double bond conversion showed only small changes with higher UV exposure, although not even one-third of complete conversion is achieved. Both, curing behavior of the front side and the reverse side indicate that the reactivity of the vinyl double bond needs to be increased to ensure complete photopolymerization and thus to reduce migration.

4 | CONCLUSIONS

In conclusion, the curing behavior of HPP-ink, containing both acrylic and vinyl double bonds, was monitored using ATR-FTIR spectroscopy. UV irradiation of HPP-ink led to changes in specific absorption bands of the FTIR spectra due to crosslinking reaction of double bonds. The peaks at 807 cm^{-1} due to C=C twisting vibration and at 1,618 to 1,636 cm^{-1} due to C=C stretching vibration decreased with UV exposure time. However, only the change in absorptions bands at 1,408 and 1,321 cm^{-1} permitted the determination of C=C conversion of acrylic and vinyl double bond, independently of one another. The relevant IR bands were determined and assigned by comparison with IR spectra of selected reference material. In addition, a method was developed which allows the investigation of surface-cure and deep-cure behavior, separately. For deep-cure investigations, the cured film was peeled off a polished stainless steel substrate using a tesafilm® stripe and the reverse side was analyzed. The conversion of acrylic double bonds increased very fast in the area of small UV dosages and then becoming more and more constant. At 691 mJ/cm^2 the acrylic portion of double bonds was almost fully consumed for the front and back side of the film. However, the reactivity of vinyl C=C bonds is markedly weaker. At 1254 mJ/cm^2 only 49% of the vinyl double bonds were crosslinked by photopolymerization at the surface of the film. On the other hand, the deep-cure conversion of the vinyl double bond reached only 30% at an irradiated UV dosage of 1,254 mJ/cm^2.

To sum up, ATR-FTIR spectroscopy allows the tracking of double bond conversion in photopolymerization reactions. Here it is possible to distinguish between surface-cure and deep-cure behavior and even between the conversion of acrylic and vinyl double bonds.

ACKNOWLEDGMENT

The authors thank Tritron GmbH for the friendly cooperation.

ORCID

Jonas Simon https://orcid.org/0000-0002-0847-0467

REFERENCES

[1] M. Graindourze, *Handbook of Industrial Inkjet Printing: A Full System Approach*, Wiley-VCH, Weinheim **2017**, p. 129.
[2] M. Prudenziati, R. Emilia, J. Hormadaly, *Printed Films*, Woodhead Publishing, Cambridge, UK **2012**, p. 3.
[3] Y. Zhang, Z. Du, X. Xia, Q. Guo, H. Wu, W. Yu, *Polym. Test.* **2016**, *53*, 276.
[4] E. A. Kandirmaz, E. N. Gençoğlu, N. Kayaman Apohan, *Macromol. Res.* **2019**, *27*, 756.
[5] S. Ji, J. Zhang, G. Tao, C. Peng, Y. Sun, R. Hou, H. Cai, *Food Packag. Shelf Life* **2019**, *21*, 100340.
[6] N. Seltenrich, *Environ. Health Perspect.* **2015**, *123*, A174.
[7] X. Fang, O. Vitrac, *Crit. Rev. Food Sci. Nutr.* **2017**, *57*, 275.
[8] S. M. Johns, S. M. Jickells, W. A. Read, L. Castle, *Packag. Technol. Sci.* **2000**, *13*, 99.
[9] W. A. C. Anderson, L. Castle, *Food Addit. Contam.* **2003**, *20*, 607.
[10] G. Sagratini, J. Mañes, D. Giardiná, Y. Picó, *J. Agric. Food Chem.* **2006**, *54*, 7947.
[11] De Mondt, R. *Radtech Rep*. **2012**, *3*, 32.
[12] C. Decker, T. N. T. Viet, D. Decker, E. Weber-Koehl, *Polymer (Guildf)* **2001**, *42*, 5531.
[13] R. W. Stowe, *Proc. SPIE* **1996**, *2831*, https://doi.org/10.1117/12.257198.
[14] G. T. Carroll, L. Devon Triplett, A. Moscatelli, J. T. Koberstein, N. J. Turro, *J. Appl. Polym. Sci.* **2011**, *122*, 168.

[15] M. Sangermano, P. Meier, IntechOpen: Rijeka, **2012**; p 16.
[16] D. Nowak, J. Ortyl, I. Kamińska-Borek, K. Kukuła, M. Topa, R. Popielarz, *Polym. Test.* **2017**, *64*, 313.
[17] K. Vikman, K. Sipi, *J. Imaging Sci. Technol.* **2003**, *47*, 139.
[18] T. Scherzer, U. Decker, *Vib. Spectrosc.* **1999**, *19*, 385.
[19] Bhargava, R.; Wang, S.-Q.; Koenig, J. L. Springer Berlin Heidelberg: Berlin, Heidelberg, **2003**; pp 137.
[20] M. Guiliano, L. Asia, G. Onoratini, G. Mille, *Spectrochim. Acta A Mol. Biomol. Spectrosc.* **2007**, *67*, 1407.
[21] D. Kunwong, N. Sumanochitraporn, S. Kaewpirom, *J. Sci. Technol.* **2014**, *33*(2), 201.
[22] A. S. G. Magalhães, M. P. A. Neto, *Quim. Nov.* **2012**, *35*, 1464.
[23] Wang, F.; Hu, J. Q.; Tu, W. P. **2008**, *62*, 245.
[24] C.-J. Chang, S.-J. Chang, F.-M. Wu, M.-W. Hsu, W. W. W. Chiu, K. Chen, *Jpn. J. Appl. Phys.* **2004**, *43*, 8227.
[25] C.-J. Chang, H.-Y. Tsai, C.-C. Hsieh, W.-Y. Chiu, *J. Appl. Polym. Sci.* **2013**, *130*, 2049.
[26] C.-J. Chang, Y.-H. Lin, H.-Y. Tsai, *Thin Solid Films* **2011**, *519*, 5243.
[27] C.-J. Chang, M.-W. Wu, C.-M. Wu, *J. Appl. Polym. Sci.* **2009**, *111*, 1391.
[28] C.-J. Chang, M.-H. Tsai, P.-C. Kao, H.-Y. Tzeng, *Thin Solid Films* **2008**, *516*, 5503.
[29] H. Kaczmarek, C. Decker, *J. Appl. Polym. Sci.* **1994**, *54*, 2147.
[30] H.-S. Joo, Y.-J. Park, H.-S. Do, H.-J. Kim, S.-Y. Song, K.-Y. Choi, *J. Adhes. Sci. Technol.* **2007**, *21*, 575.

How to cite this article: Simon J, Langenscheidt A. Curing behavior of a UV-curable inkjet ink: Distinction between surface-cure and deep-cure performance. *J Appl Polym Sci*. 2020;137: e49218. https://doi.org/10.1002/app.49218